Acupuncture & Electro-Therapeutics Research, The International Journal
Vol. 33(3-4), pp.169-78, (2008)

Heat Transfer Involved in a Warm (Moxa-Heated) Needle Treatment

Vincent C. Huang, Ph.D., Post-Doctoral Fellow
Department of Engineering Sciences and Ocean Engineering, National Taiwan University,
No. 1, Sec. 4, Roosevelt Road, Taipei, 10617 Taiwan
Tony W.H. Sheu, Ph.D., Professor
Department of Engineering Sciences and Ocean Engineering, National Taiwan University,
No. 1, Sec. 4, Roosevelt Road, Taipei, 10617 Taiwan

Correspondence: Tony W. H. Sheu; Department of Engineering Sciences and Ocean Engineering, National Taiwan University, No. 1, Sec. 4, Roosevelt Road, Taipei, 10617, Taiwan;
Tel: +886-2-33665746; Fax: +886-2-23929885; E-mail: twhsheu@ntu.edu.tw

(Received: May 21, 2008; Accepted with Revisions May 23 2008)

ABSTRACT:

A numerical study has been performed to reveal the temperature distributions in tissues around the GB38 acupoint during the acupuncture with a burning moxibustion placed on the top of the handle of the acupuncture needle (called as the warm needle treatment, WNT, in the present study). The proposed WNT model involves needle, needle handle and calf section around the GB38 acupoint. For validating the numerical results, experiment by virtue of the calibrated infrared (IR) camera was also conducted. Our aim is to calculate the skin surface temperature and the temperatures under warm needle at different depths beneath the skin. From the temperature profile along the centerline of the acupuncture needle, the temperature is seen to decrease rapidly from the burning moxa section (200 ºC) to the skin surface (36 ºC). The temperature near the needle (36 ºC) is only 1 ºC higher than those predicted at other places (~35 ºC). This phenomenon explains why this

treatment practice is called as the warm needle rather than the hot needle.

Key Words: Acupuncture; Moxibustion; Warm needle; Infrared

Introduction

Acupuncture, which is among the oldest healing practices in the world, was originated from the traditional Chinese medicine (TCM). Acupuncture is meant to stimulate some of the specific points in the body by a variety of techniques, including an insertion of thin metal needles into the skin, with an aim to remove blockages or restore and maintain human health. Acupuncture is now accepted as a part of complementary and alternative medicines and has been practiced in many medical and health care systems.

Warm needle is an important acupuncture technique in TCM. There is a traditional saying: “first you use the needle (acupuncture); then the fire (moxibustion) and finally the herbs” [1]. Moxibustion rather than acupuncture has been chosen to cure severe diseases, in particular, due to vacuity cold and Yang deficiency. However, the very hot moxibustion applied on the skin surface is hard to get rid of the scald. The underlying idea of warm needle in Chinese literature is to combine the acupuncture and moxibustion into a single treatment, which enjoys the functions of both (acupuncture and moxibustion) but can avoid the pain due to moxibustion. Since it has the safe, efficient and less painful characteristics, warm needle becomes the popular therapy nowadays.

Materials and methods

During treatment, a dried and pounded moxa is attached to the handle of the acupuncture needle after the needle being inserted into the acupuncture point. This is followed by igniting the moxa and keeps it burning (Fig. 1). Typically, the distance between the skin surface and the burning moxa stick is about 2 cm. Heat will be conducted from the needle handle to the needle itself and, finally, to the surrounding tissues. This acupuncture design with a burning moxa can maintain a temperature gradient across the needle and enhance the Seebeck effect [2]. In Chinese medicine theory, this method is highly appropriate for use to patients with vacuity cold and wind damp [3] since it can provide the functions of warming the meridians and promote the qi- and blood-flow. This therapy is also applicable to release cold-damp syndrome for the patients with rheumatoid arthritis [4]. The other technique described in the classics is called the fire needle, which involves holding the needle in a lamp flame until it becomes very hot. The procedure is followed by inserting the needle to the appropriate depth in the body quickly and then removing it [5]. In comparison with the fire needle, the warming needle allows a longer retention and a

gentler heating. In this study, we will present the thermal analysis on a warm needle and predict the temperature distribution near the curing point. Our hope is to offer a better way to understand the traditional Chinese medical theory.

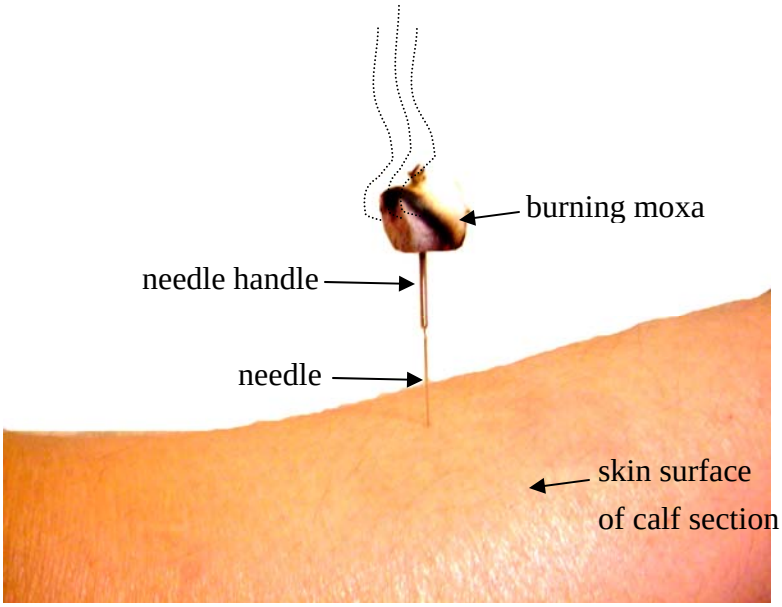

Fig. 1: Schematic of the warm needle inserted to the acupoint.

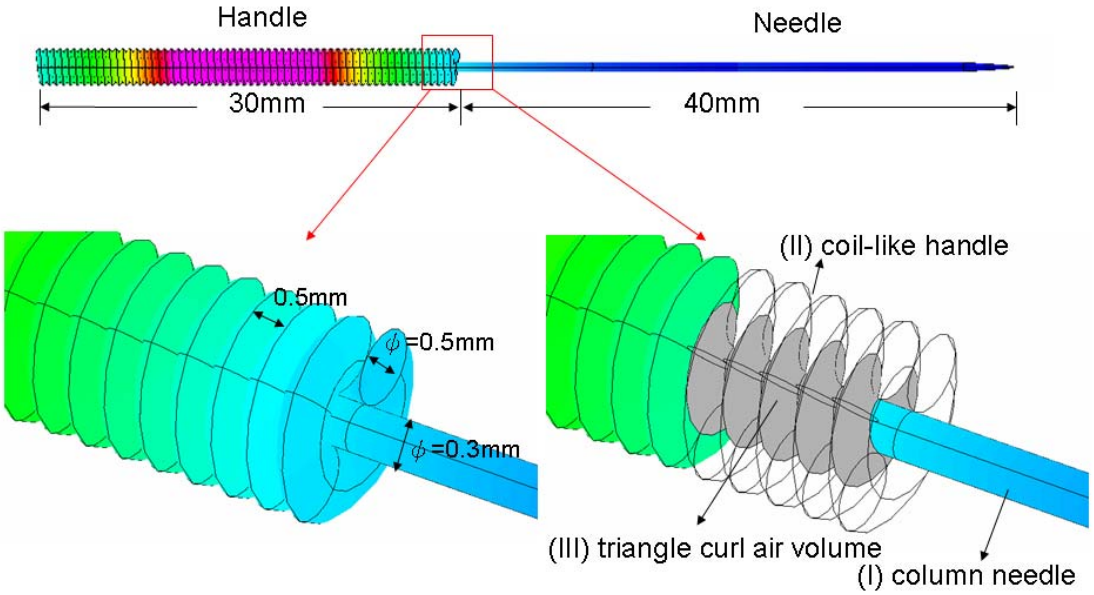

Fig. 2: Acupuncture needle is composed of one-column needle (portion I) and one coil-like handle (portion II), which covers the column needle.

A needle assembly for acupuncture includes a column needle (portion I) with its head having a sharp end and one coil-like handle (portion II), which covers the dull end of the column needle (Fig. 2). Between the column needle and the coiled handle, there exists a triangle air

volume (portion III). Fig. 2 shows the investigated 1.5-inch acupuncture needle and the sizes of different parts. A hybrid mesh system, containing both of the structured- and unstructured-type meshes shown in Fig. 3, is generated from the total number of 7,421 mesh points. The mesh density has been properly distributed in this study so that the predicted solutions can accurately represent the physical phenomenon.

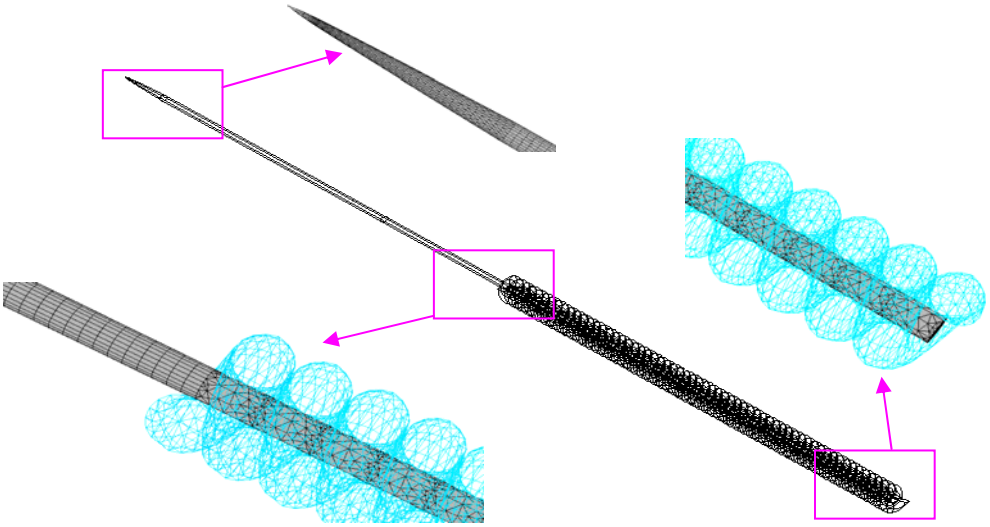

Fig. 3: The surface mesh generated on the acupuncture needle.

Heat transfer process is predicted by solving the equation for energy conservation. In this study, the energy equation cast in the form of total enthalpy below will be employed

$$\frac{\partial(\rho h_0)}{\partial t}+\nabla\cdot(\rho\vec{V}h_0)=\nabla\cdot(k\nabla T)+\frac{\partial p}{\partial t}+[\frac{\partial(u\tau_{xx})}{\partial x}+\frac{\partial(u\tau_{yx})}{\partial y}+\frac{\partial(u\tau_{zx})}{\partial z}]$$

$$+[\frac{\partial(v\tau_{xx})}{\partial x}+\frac{\partial(v\tau_{yx})}{\partial y}+\frac{\partial(v\tau_{zx})}{\partial z}]+[\frac{\partial(w\tau_{xx})}{\partial x}+\frac{\partial(w\tau_{yz})}{\partial y}+\frac{\partial(w\tau_{zz})}{\partial z}] \quad (1)$$

In the above, h_0 is the total enthalpy defined as

$$h_0=i+\frac{p}{\rho}+\frac{1}{2}(u^2+v^2+w^2) \quad (2)$$

and i, k, p and τ_{ij}, denote the internal energy, thermal conductivity, static pressure and viscous stress tensors. In addition, u, v, w and $\vec{V}$ are the flow velocities along the x, y, z directions and the flow velocity vector, respectively.

Simulation of equation (1) will be carried out by employing the commercially available

finite volume package, namely, CFDRC [6]. This software package includes the CFD-GEOM for geometry and grid generation, the CFD-ACE$^+$ for solution solver and the CFD-VIEW for post-processing. A convenient graphical user interface (GUI) is also provided for specifying the physical properties under investigation, and the specification of the boundary and initial conditions. In CFD-ACE$^+$ solver, the finite volume method is employed together with the algebraic multigrid method and the conjugate gradient squared solution solver for purposes of accelerating calculation. In this study, the central difference scheme has been selected to approximate the parabolic type partial differential equation (PDE).

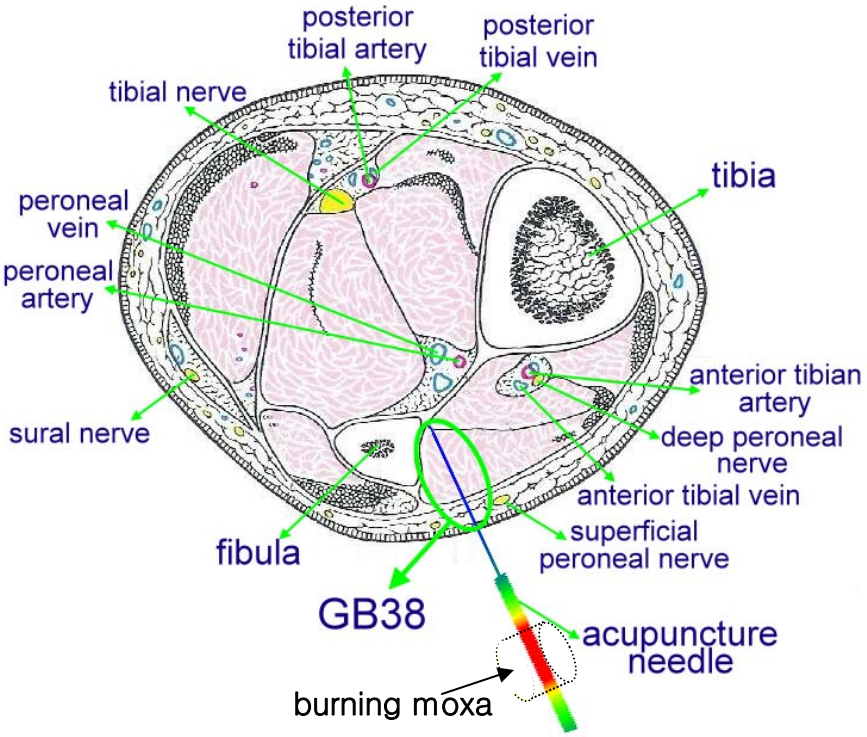

Fig. 4: Schematic of the axial image of the right leg for the GB38 acupuncture point (Courtesy of Yang [7]).

GB38 is one of the acupuncture points in gall bladder (GB) meridian, which can deal with hemicrania and joints ache. Fig. 4 shows the axial image of the right leg for the GB38 acupuncture point (Courtesy of Yang [7]). At the calf section, the amount of capillaries near the GB acupuncture points is greater in number than those at the other parts of the body [8]. This characteristic suggests that the GB meridian has a larger potential in acupuncture research. Also, the distances between the acupoints GB37-GB38 and GB38-GB39 are about the same (about an inch). Therefore, the acupoint GB38 was the focus of other [9, 10, 11] and the current studies. The boundary conditions applied on the calf section with needle are shown in Fig. 5, where BC I, II and III represent the isothermal, symmetric and convection- type boundary conditions, respectively. BC Ia shows the boundary of needle handle which carries moxa (moxa cone of 1

cm diameter and 1cm length, which was made by the dried Artemisia vulgaris leaves with a weight of 100 mg) and has the same temperature (200 ^{o}C) as the burning moxa. The temperatures in the bone zone (BC Ib), including fibula and tibia, are specified as 37 ^{o}C to simulate the human body temperature. The symmetric conditions at the upper and bottom sides of calf section (BC II), which connects with knee and foot, are specified to account for the same structures of muscle tissues with knee and foot. BC III is normally chosen to simulate the transfer of heat to/from the surrounding (i.e., the area outside of the computational system) by convection. This subtype is used to fix either the wall temperature or the heat flux. On the wall of BC III, it is prescribed by the following equation

$$q_w = h(T_E - T_w) \tag{3}$$

where h and T_E denote the heat transfer coefficient and the surrounding temperature. The wall temperature (T_w) is unknown and will be determined by balancing the heat fluxes between the surrounding and the model surface.

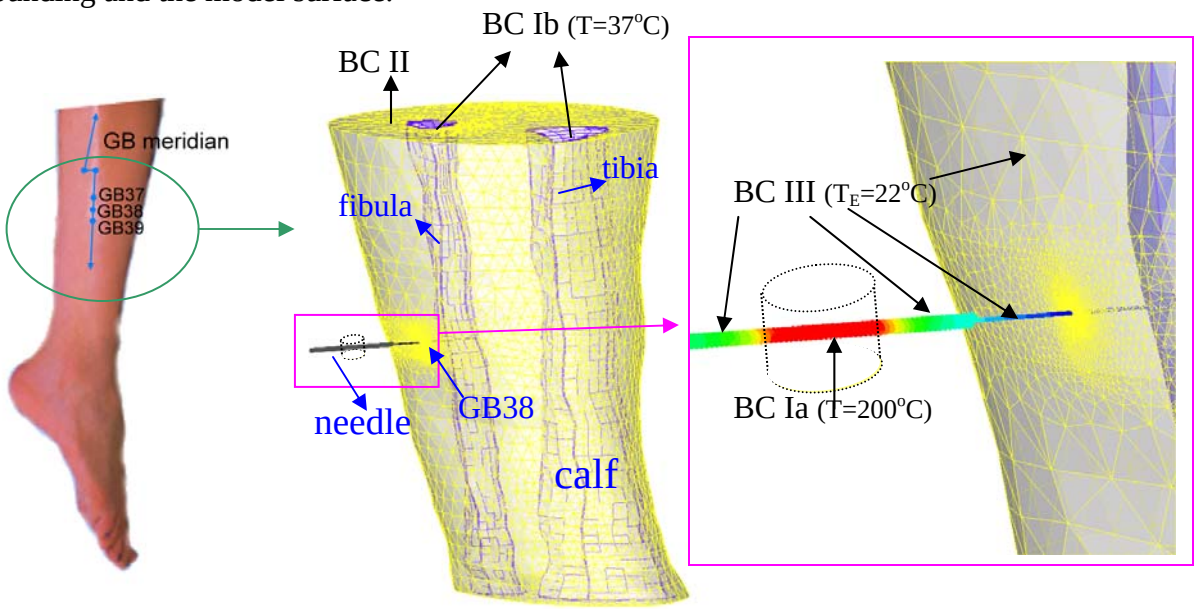

BC Ia: isothermal (T=200 ^{o}C) BC Ib: isothermal (T=37 ^{o}C)
BC II: symmetry BC III: external heat transfer (by convection)

Fig. 5: Schematic of the boundary conditions for the acupuncture needle being inserted to the acupoint GB38.

The current study employs 25,872 nodal points to generate the mesh shown in Fig. 5. The mesh densities have been kept increasing until the computed solutions become grid-independent. In all the iterative processes, calculation of the enthalpy values will be terminated when their

residual norms become smaller than 10^{-15}.

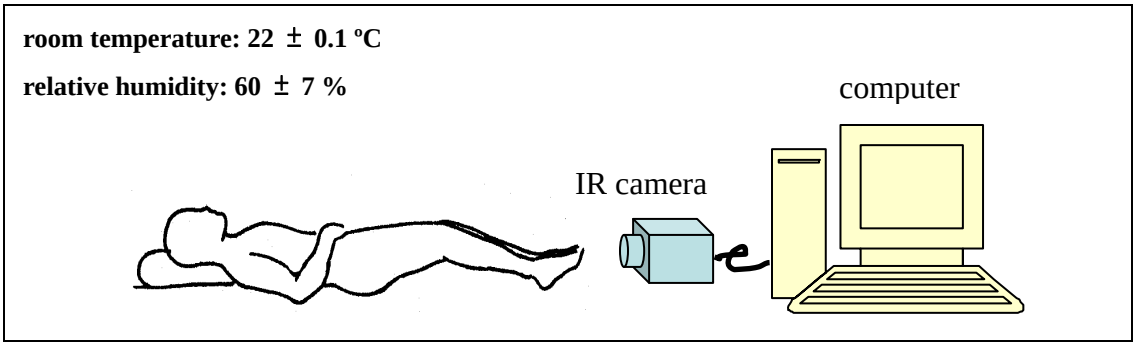

Fig. 6: The IR image recording was used to take pictures during moxibustion treatment on the human GB38 acupoint. The recording IR images will then sent to the computer.

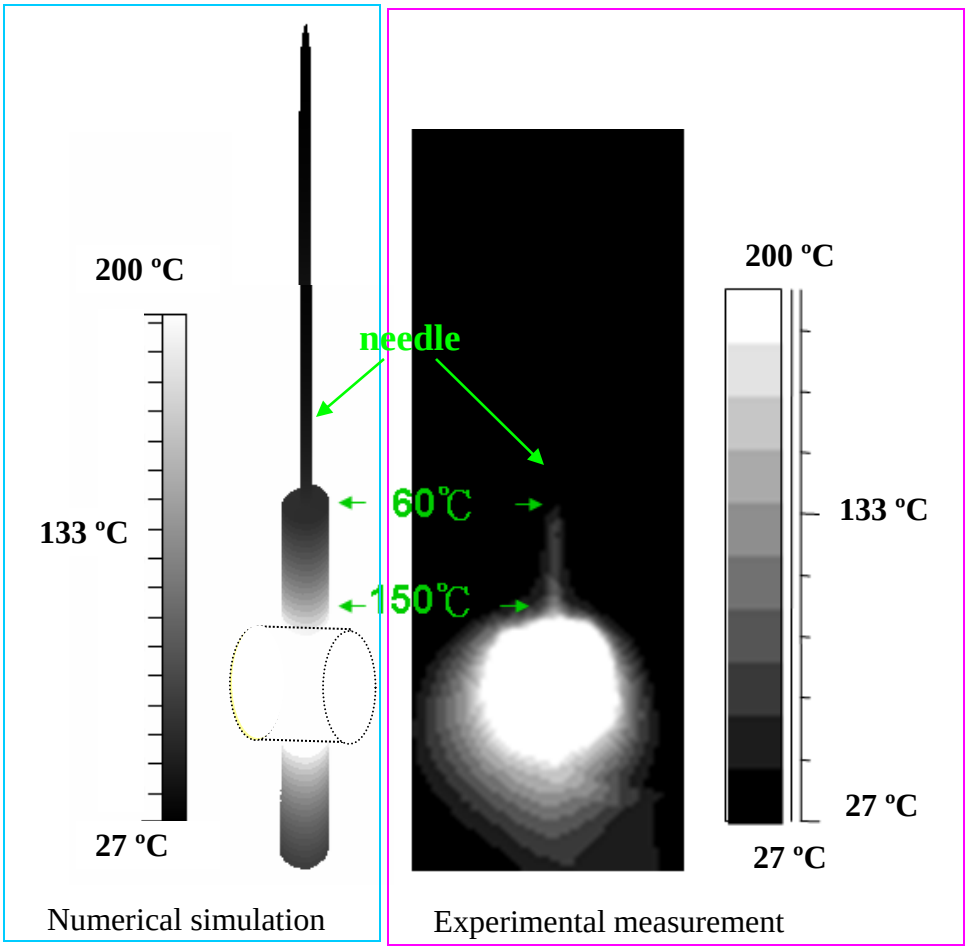

Fig. 7: Comparison of the numerically predicted and the experimentally measured temperatures for the burning moxa stick applied on the handle of the acupuncture needle. The temperature of burning moxa is 200 ºC. Temperature gradient will be established across the needle, starting from the needle handle and ending at the needle head.

Results

In order to know the temperature distribution resulting from the burning moxa, IR image recording has been performed under the monitor light. The schematic diagram of this experiment is shown in Fig. 6. The IR image recording system we used is known as the FLIR system (ThermaCAM® SC500 from FLIR Systems TM) [12], which includes an IR camera for acquiring IR images, a computer with FLIR software for data analysis. Both of the camera and the subject are kept apart from the external draft IR sources. The room temperature and the relative humidity are kept at 22 ± 0.1 ºC and 60 ± 7 %, respectively. Thermography has been carried out with a calibrated IR camera, which is equipped with a 45º close-up optic. Sensitivity, accuracy and resolution for the employed camera are 0.07 ºC, ± 2 ºC and 320 × 240 pixels, respectively. The distance between the camera and the subject under current investigation is 0.1 m. The infrared images of the subject, at a sampling rate of 4 Hz, are directly recorded in the computer's hard disk.

k_s	16 W/m ºC	Thermal conductivity of the stainless steel
k_c	$0.4574 + 0.001403T$ W/m ºC	Thermal conductivity of the calf
k_a	0.0299 W/m ºC	Thermal conductivity of the air
Cp_s	460 J/kg ºC	Specific heat of the stainless steel
Cp_c	3,594 J/kg ºC	Specific heat of the calf
Cp_a	1,009 J/kg ºC	Specific heat of the air
ρ_s	7,800 kg/m^3	Density of the stainless steel
ρ_c	1,035 kg/m^3	Density of the calf
ρ_a	1.0 kg/m^3	Density of the air
h_s	7.9 W/m^2 ºC	Heat transfer coefficient of the stainless steel
h_c	3.7 W/m^2 ºC	Heat transfer coefficient of the calf
T_E	22 ºC	Environment temperature
T_m	200 ºC	Moxa burning temperature
T_B	37 ºC	Human body temperature

Table 1: The physical properties employed in the present simulation study.

In TCM, acupuncture needle can be made from stainless steel, iron, copper, silver and pottery etc. For the reasons of safety and cost effectiveness, stainless steel is now more popular.

This study employs the normal stainless steel needle (1.5 inch needle, 7 cm total length with 3cm length in the needle handle part) in the experiments and numerical simulations. The thermal conductivity, specific heat, density and heat transfer coefficient of the stainless steel are denoted as k_s, Cp_s, ρ_s and h_s, respectively. At the normal state with the room temperature (22 ºC in this study), these coefficients are prescribed with the values of k_s = 16 W/m ºC, Cp_s = 460 J/kgºC, ρ_s = 7,800 kg/m^3 and h_s = 7.9 W/m^{2}ºC [13], respectively. The other associated coefficients are tabulated in Table 1. The predicted convergent temperature, which is plotted in Fig. 7, on the needle surface is seen to distribute similarly to the experimentally measured values by IR image.

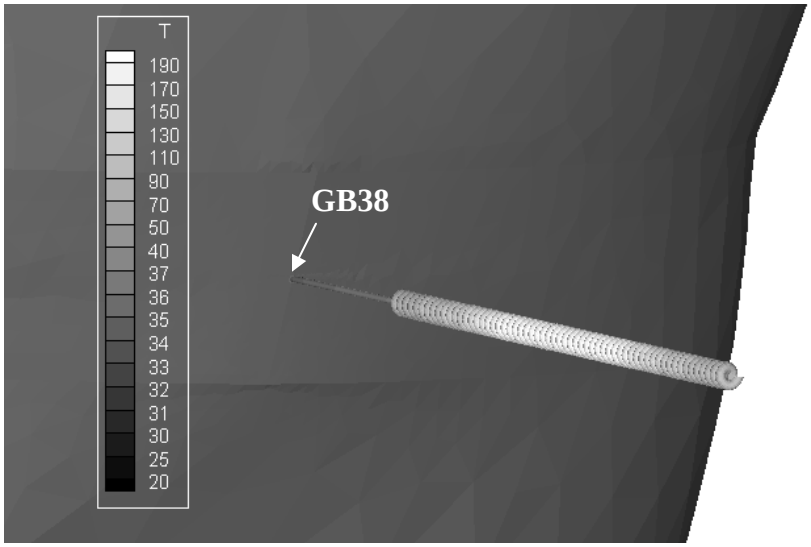

Fig. 8: The predicted skin surface temperature contours for the warm needle applied at the acupoint GB38.

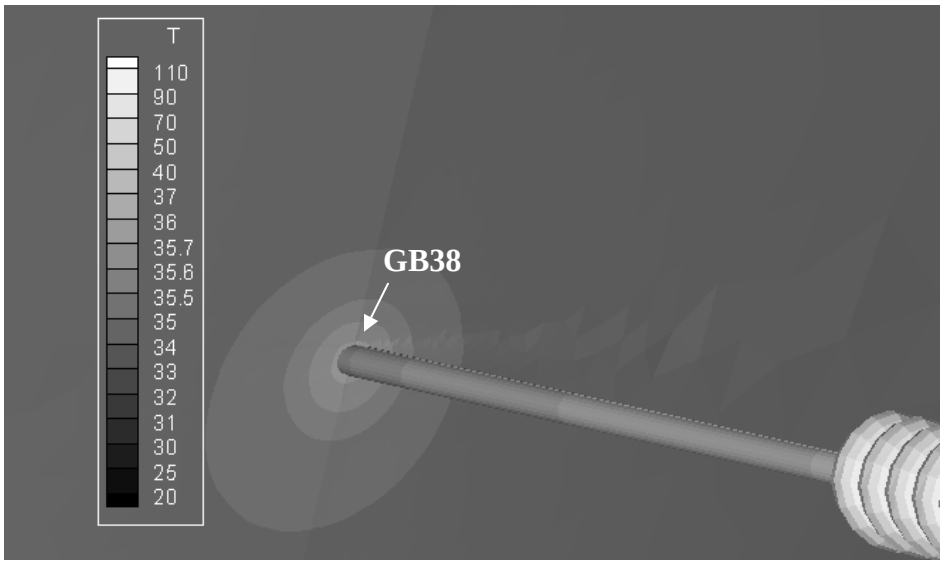

Fig. 9: The predicted skin surface temperature contours at an area very near the acupoint GB38.

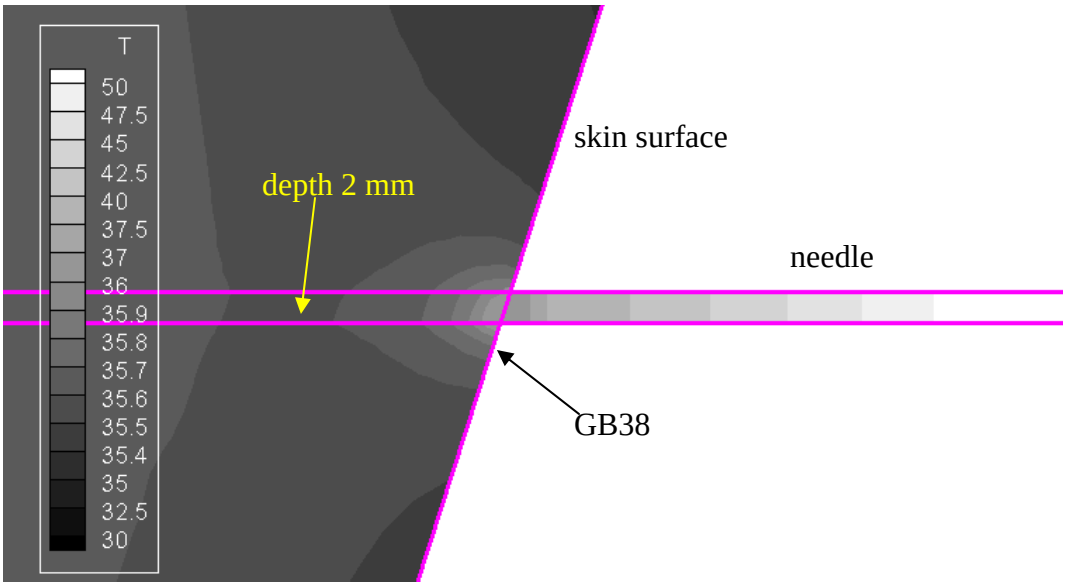

Fig. 10: The predicted temperature contours on the cutting plane, which passes through the acupoint GB38.

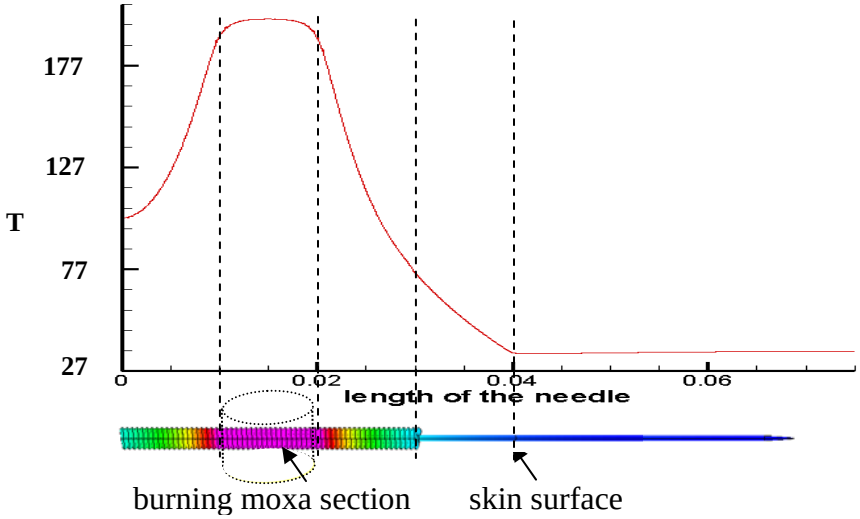

Fig. 11: The predicted temperature distribution along the centerline of the acupuncture needle for a warm needle applied at the acupoint GB38.

Fig. 8 shows the predicted temperature contours near the acupoint GB38 under the warm needle treatment. Around the skin surface of GB38 (Fig. 9), the surface temperature near the needle is predicted to be about 36 ºC, which is 1 ºC higher than those predicted at other skin surfaces (~ 35 ºC). Fig. 10 shows the predicted temperature contours on the cutting plane passing through the acupuncture needle and GB38 acupoint. The tissue temperature around the needle is

only 1 ºC higher than others. Since the needle is smaller in comparison with the human body, the effect of burning moxa on needle handle is relatively less significant. In TCM, warm needle is involved in the acupuncture with burning moxa. From Figs. 9 and 10, we can understand why this treatment isn't called as the hot needle, even the temperature of the burning moxa can be as high as 200 ºC. Fig. 11 shows the predicted temperature profile along the center line of the acupuncture needle. From this profile, we can see that the temperature can be varied from 200 ºC (burning moxa section) to 36 ºC (skin surface) in a short length of 2 cm. We can also find that the temperatures at locations beneath the skin surface of depths 0 mm, 1 mm, 2 mm, 3 mm and 4 mm are 36.00 ºC, 35.63 ºC, 35.59 ºC, 35.62 ºC and 35.66 ºC, respectively.

Discussion

In the present study, both the experimental measurement and the numerical simulation have been conducted to know the temperature distribution near the acupoint which is subjected to a warm needle. The predicted temperature contours on the needle surface are shown to agree well with the experimentally measured results. Moreover, the temperature contours of the tissues beneath of the skin surface have been also numerically predicted. From the temperature profile along the centerline of the acupuncture needle, the temperature decreases very rapidly from the burning moxa section (200 ºC) to the skin surface (36 ºC). The temperature near the needle is only 1 ºC higher than those predicted at other places. The predicted phenomenon explains why this treatment skill is called as the warm needle rather than the hot needle. These results are fundamentally important to the study of TCM.

Acknowledgments

The authors will acknowledge Prof. Ping-Hei Chen from Department of Mechanical Engineering, NTU, Taiwan, who provided the FLIR system for the temperature measurements.

References

1. Tsuei, J. J., "The science of acupuncture－theory and practice." IEEE Engineering in Medicine and Biology. May/June, pp. 52–57, 1996.
2. Cohen, M., Kwok, G., and Cosic, I., "Acupuncture needles and the Seebeck effect: do temperature gradients produce electro-stimulation?" Acupuncture and Electro -therapeutics Research. Vol. 22, pp. 9-15, 1997.
3. Wiseman, N., and Feng, Y., A Practical Dictionary of Chinese Medicine. Paradigm Publications, Brookline, MA, pp. 664, 1998.
4. Li, C., Jiang, Z., and Li, Y., "Therapeutic effect of needle warming through moxibustion at twelve shu points on rheumatoid arthritis." Journal of Traditional Chinese Medicine. Vol

19(1), pp. 22-26, 1999.

5. Unschuld, P. U., Introductory Readings in Classical Chinese Medicine. Kluwer Academic Publishers, Dordrecht, Holland, 1988.
6. CFD-ACE-GUI User Manual Volume II. CFD Research Corporation, pp. 85-94, 2003.
7. Yang, J.K., Meridian Cross-section Anatomy. Shang Hai Science Technology Press, Chinese, pp. 76, 1997.
8. Fei, L., "Researches and developments of meridian physical basic and function experiments." Chinese Science Bulletin. Vol 43(6), pp. 658-672, 2000.
9. Sheu, T.W.H. and Huang, V.C., "Development of an electro osmotic flow model to study the dynamic behavior in human meridian." International Journal for Numerical Methods in Fluids. Vol 56, 739–751, 2008.
10. Huang, V.C. and Sheu, T.W.H., "On a dynamical view on the meridian transmission." Journal of Accord Integrative Medicine. Vol.4(2), pp.97-107, (2008).
11. Huang, V.C. and Sheu, T.W.H., "Tissue fluids in microchannel subjected to an externally applied electric potential." International Journal for Numerical Methods for Heat & Fluid Flow. in press (2007.11 accepted).
12. ThermaCAM SC500 Operator's Manual. FLIR Systems, 1999.
13. The engineering toolbox. Tools and Basic Information for Design, Engineering and Construction of Technical Applications, http://www.engineeringtoolbox.com/.